Spatial organization and gene expression changes affected by smoking in the tumor microenvironment in head and neck squamous cell carcinomas

Kirsteen H. Maclean; Lakshmi Chandramohan; Maryam Rohafza; Harry Nunns; Erinn Parnell; Qingyan Au; Anna-Juncker-Jensen

NeoGenomics Laboratories

AACR 2024 #5494

Background: Oral squamous cell carcinoma (OSCC) is the most common head and neck cancer and accounts for over 90% of cancers that develop within the mucosal epithelium of the oral cavity. Additional carcinogenic risk factors, including tobacco, alcohol and HPV infection are also associated with the pathogenesis of oral carcinogenesis. Unfortunately, today the failure of standard treatment modalities, such as surgery, radiotherapy, and chemotherapy underscore the need to identify better biomarkers of this disease. Advances, especially in spatial technology have created unprecedented opportunities to identify cell types and biomarkers of disease processes, revealing important relationships within the tumor microenvironment (TME) that allow a detailed characterization of specific cell phenotypes defined by co- or lack of expression of multiple markers that may help in predicting clinical responses and mechanisms of resistance to therapy. To better understand the effects of smoking use and potential changes within the TME, a cohort of OSCC tumors +/- a history of smoking was analyzed using a proprietary comprehensive spatial workflow coupled to gene expression analysis.

Methods: A retrospective analysis was performed on biopsied FFPE samples from OSCC patients with and without a history of smoking and treated +/- chemotherapy. Specifically, patient samples representing OSCC-smokers were compared to samples derived from OSCC tumors-non-smokers. In order to perform a comprehensive expression profiling of the TME from OSCC tumors we used transcriptomic information from bulk mRNA gene expression acquired using the NanoString nCounter® PanCancer IO 360™ panel (**Figure 1**) that includes the Tumor Inflammation Signature (TIS), as well as targets that characterize immune hot, desert, and cold regions in the stroma and tumor epithelium. To correlate some of the gene expression data and derive spatial insights, we used the spatial MultiOmyx™ immunofluorescence (IF) multiplexing assay, **Figure 2** (NeoGenomics Laboratories, Inc.).

Results: We comprehensively characterized gene expression and the spatial landscape of several immune markers in OSCC samples and further investigated the relationship of smoking status to biomarker expression by examining the cell composition and overall immune changes within the tumor immune microenvironment. A better understanding of the TME and the effect of smoking in head and neck tumors will allow us to better tailor the treatment of patients to continue to improve outcomes.

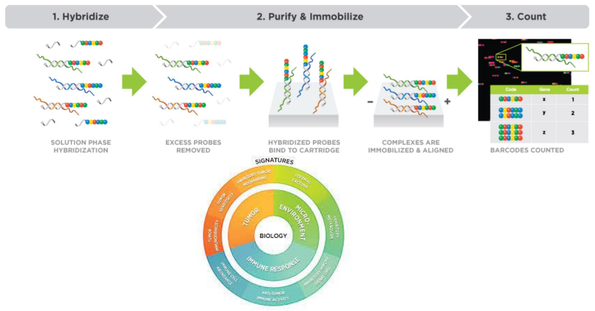

Figure 1: nCounter® workflow and PanCancer IO 360™ panel

MultiOmyx Analysis of Immune Populations

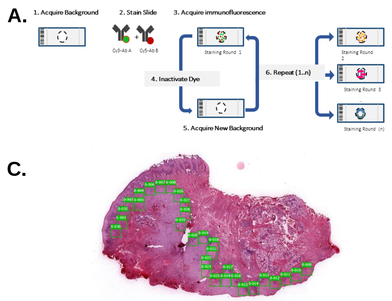

Co-expressions	Phenotype
CD3+CD4+	T helper
CD3+CD4+FoxP3+	T regulatory
CD3+CD8+	Cytotoxic T cell
CD3-CD20+	B cell
CD3-CD56+	NK cells
CD68+CD163+	M2 TAM
CD68+CD206+	M2 TAM
CD68+arginase+	M2 TAM
CD31+Cladin6+	Claudin6+ endothelial
PanCK+Claudin6+	Claudin6+ tumor
PanCK+Ki67+	Proliferating tumor

Figure 2. **(A).** Project workflow. Two conjugated fluorescent antibodies are applied per imaging round followed by image acquisition of the stained slides. The dye is then erased, enabling a subsequent round of staining. Once imaging is complete, AI algorithms segment and phenotype cells. **(B).** Composition of 14-marker panel. **(C).** Representative H&E with ROIs selected for imaging and analysis indicated in green.

Differential Expression: Smokers vs non-Smokers

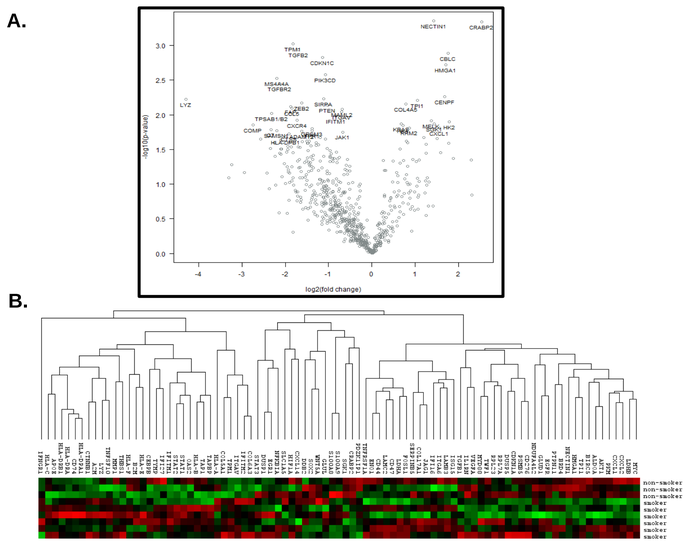

Figure 3: **(A).** Volcano Plot. Linear regression differential expression in smokers vs baseline of non-smokers. Genes displayed on the left and right correspond to those targets with the greatest decreased or increased expression. **(B)**. Heatmap. Top expressed targets are clustered by smoking status. Green represents low and red a higher expression level.

Impact of Smoking on Cellular Composition

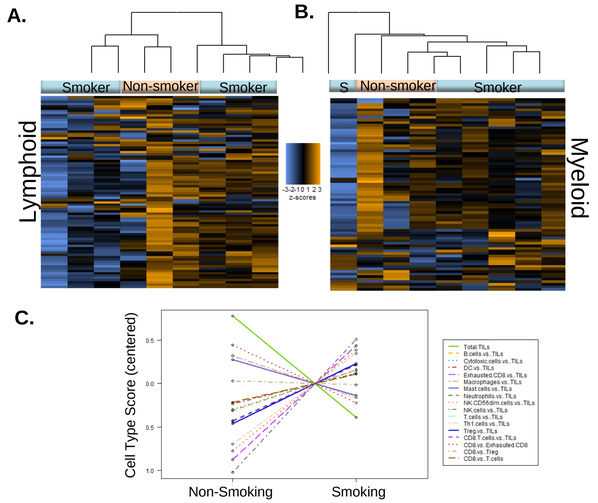

Figure 4: (A). Lymphoid cell types **(B)**. Myeloid cell types. Heatmap of relative cell type measurements showing the abundance of different cell types. Orange indicates high abundance whereas blue indicates low abundance. **(C)**. Centered cell type score. Raw cell type abundance measurement vs smoking status.

Cell Type Profiling

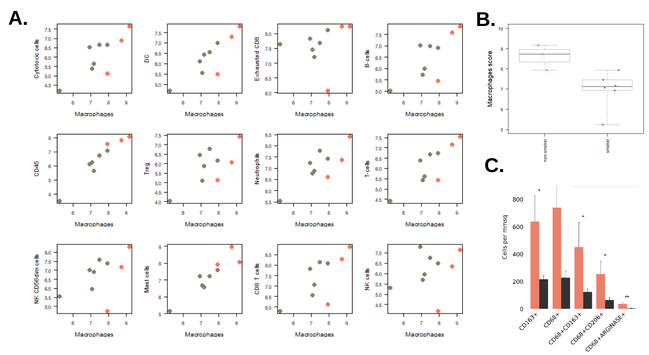

Figure 5: (A). Each panel plots macrophages vs raw abundance measurement of other cell types . Points are colored by non smoker (Red), smoker (Grey). **(B)**. Macrophage measurements in smokers vs non-smokers. **(C)**. MultiOmyx NeoLYTX Spatial Analysis quantifies the prevalence of specific macrophage subsets in smokers vs non-smokers

MultiOmyx Analysis & Images

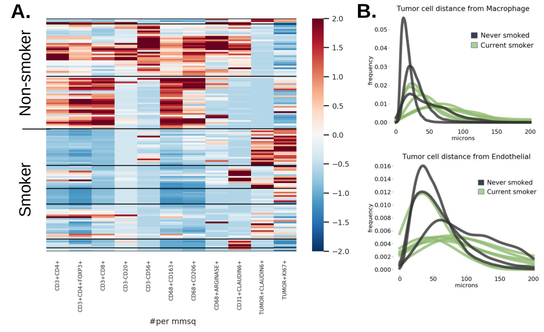

Macrophage Characterization

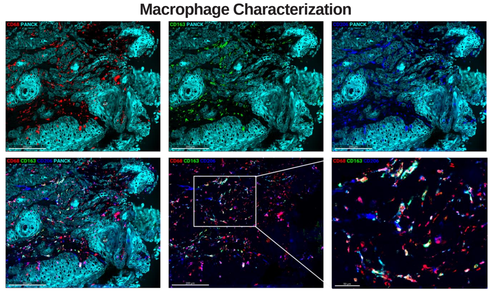

Tumor Proliferation, T cells & Endothelium

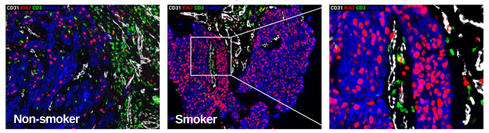

Figure 5: (A). Protein density heatmap. **(B)**. MultiOmyx NeoLYTX Nearest Neighbor Analysis of the TM, for non-smokers vs smokers. **(C)**. Representative color overlays of macrophages in a tumor from a smoker (top panel), and tumor proliferation in tumors from a non-smoker and a smoker (bottom panel).

Key Take-Aways

- OSCC of the non-smokers (NS) appears to be a distinct type of tumor, with a more immunogenic TME.
- Higher number of macrophages in the NS group detected by both IO360 gene analysis and MultiOmyx spatial analysis.
- NS demonstrated an increase in the production of pro-inflammatory cytokines, e.g. interleukins and chemokines.
- These results may help to improve the treatment of OSCC in non-smokers

anna.Juncker-jensen@neogenomics.com

kirsteen.maclean@neogenomics.com